

Progresses in FAZIA detection system and preliminary results from the ISO-FAZIA experiment

G. PASTORE⁽¹⁾⁽²⁾, S. PIANTELLI⁽²⁾, D. GRUYER⁽²⁾, L. AUGEY⁽³⁾, S. BARLINI⁽¹⁾⁽²⁾, R. BOUGAULT⁽³⁾, M. BINI⁽¹⁾⁽²⁾, A. BOIANO⁽¹¹⁾, E. BONNET⁽⁵⁾, B. BORDERIE⁽⁴⁾, M. BRUNO⁽⁹⁾, G. CASINI⁽²⁾, A. CHBIBI⁽⁵⁾, M. CINAUSERO⁽⁶⁾, D. DELL'AQUILA⁽¹⁰⁾⁽¹¹⁾, J. A. DUEÑAS⁽¹²⁾, Q. FABLE⁽⁵⁾, D. FABRIS⁽⁶⁾, L. FRANCALANZA⁽¹⁰⁾⁽¹¹⁾, J. D. FRANKLAND⁽⁵⁾, F. GRAMEGNA⁽⁶⁾, M. HENRI⁽³⁾, A. KORDYASZ⁽⁷⁾, T. KOZIK⁽⁸⁾, R. LA TORRE⁽¹⁰⁾⁽¹¹⁾, N. LE NEINDRE⁽³⁾, I. LOMBARDO⁽¹¹⁾, L. O. LOPEZ⁽³⁾, J. MABIALA⁽⁶⁾, T. MARCHI⁽⁶⁾, L. MORELLI⁽⁹⁾, A. OLMI⁽²⁾, M. PÂRLOG⁽³⁾, G. PASQUALI⁽¹⁾⁽²⁾, G. POGGI⁽¹⁾⁽²⁾, F. SALOMON⁽⁴⁾, A. A. STEFANINI⁽¹⁾⁽²⁾, S. VALDRÈ⁽¹⁾⁽²⁾, G. TORTONE⁽¹¹⁾, E. VIENT⁽³⁾, G. VERDE⁽⁴⁾, M. VIGILANTE⁽¹⁰⁾⁽¹¹⁾, R. ALBA⁽¹³⁾, C. MAIOLINO⁽¹³⁾ and D. SANTONOCITO⁽¹³⁾

⁽¹⁾ Dipartimento di Fisica, Università di Firenze - Firenze, Italy

⁽²⁾ INFN, Sezione di Firenze - Sesto Fiorentino (FI), Italy

⁽³⁾ LPC Caen, Normandie Univ, ENSICAEN, UNICAEN, CNRS/IN2P3 - Caen, France

⁽⁴⁾ Institut de Physique Nucléaire, CNRS/IN2P3 - Université Paris-Sud 11 - Orsay, France

⁽⁵⁾ GANIL, CEA/DSM-CNRS/IN2P3 - Caen, France

⁽⁶⁾ INFN, LNGS Legnaro - Legnaro (PD), Italy

⁽⁷⁾ Heavy Ion Laboratory, University of Warsaw - Warsaw, Poland

⁽⁸⁾ Jagiellonian University, Institute of Physics - Krakow, Poland

⁽⁹⁾ INFN, Sezione di Bologna - Bologna, Italy

⁽¹⁰⁾ Dipartimento di Fisica, Università di Napoli "Federico II" - Napoli, Italy

⁽¹¹⁾ INFN, Sezione di Napoli - Napoli Italy

⁽¹²⁾ Departamento de Ingeniería Eléctrica, Universidad de Huelva - Huelva, Spain

⁽¹³⁾ INFN, Laboratori Nazionali del Sud - Catania, Italy

received 10 January 2017

Summary. — In this contribution the status of the FAZIA project is presented, with a particular focus on the first experiment (identified as ISO-FAZIA) after the R&D phase. In this experiment four complete FAZIA blocks in a fully operating configuration were used. They were mounted in a planar "belt" geometry, symmetrically positioned with respect to the beam axis, covering the polar angles between 2.5° and 17.4° degrees. The investigated systems were $^{84}\text{Kr} + ^{48,40}\text{Ca}$ at 35 AMeV. The main goal of the experiment was the study of the isospin transport phenomena, extending a previous analysis. This contribution will report on the isotopic identification capability of the FAZIA detector as well as preliminary results concerning the average isospin of the quasi-projectile produced in semiperipheral collisions as a function of the isospin of the target.

1. – Introduction

Since almost ten years the FAZIA collaboration [1] has been involved in the design and construction of a multidetector array based on Si-Si-CsI telescopes with high performances in terms of isotopic identification, mainly devoted to the range of the Fermi energy (25–35 AMeV). The principal purpose of the R&D phase of FAZIA was the optimization of different identification techniques, in order to study isospin transport phenomena and symmetry energy term far from normal conditions [2-4]. In particular the main effort of the collaboration was dedicated to the improvement of the traditional $\Delta E-E$ and the Pulse Shape Analysis (PSA) techniques. The PSA is a very interesting technique allowing the lowering of energy thresholds for the identification of charged fragments. Correlating the detected energy with a parameter related to the signal shape, it is possible to obtain the identification also for particles stopped inside the first layer of the telescope [5, 6].

In a previous work [2] we studied the isospin transport phenomena using the reactions $^{84}\text{Kr} + ^{112,124}\text{Sn}$ at 35 AMeV with a single prototype telescope having a reduced angular coverage thus permitting only inclusive measurements. The isospin diffusion was observed looking at the products coming from the Quasi-Projectile (QP) in the two reactions: a higher $\frac{\langle N \rangle}{Z}$ content has been found for the ^{124}Sn target. Also a hint of isospin drift was observed studying the $\frac{\langle N \rangle}{Z}$ as a function of the fragment velocity for the different elements: light fragments show a dependence on the velocity (the $\frac{\langle N \rangle}{Z}$ ratio increases moving from the QP velocity region to the midvelocity one) in full agreement with many previous finding [3, 4]. In fact, the isospin drift consists in the n-enrichment of the “neck” region between the two nuclei. Only particles and fragments coming from this neck region can keep memory of such process.

The goal of the ISO-FAZIA experiment is an extension of our previous study [2] exploiting a better detector performance in terms of isotopic identification (for example the PSA with mass discrimination on the first silicon layer) and a higher angular coverage. In this way we can investigate also coincidence events, when a QP fragment is detected with some accompanying light particles or fragments. Therefore we can then explore the evolution of the neutron contents of these lighter partners using velocity and angular correlations and with some cuts on the QP properties (size and center of mass velocity).

2. – Experimental setup

The reaction $^{80}\text{Kr} + ^{48,40}\text{Ca}$ at 35 AMeV has been performed in Catania at Laboratori Nazionali del Sud (LNS), INFN. The grazing angles in the laboratory frame are around 1.9° . We used 4 complete FAZIA blocks (see sect. 2.1) in a belt configuration covering an angle from 2.5° to 17.4° around the beam, slightly out of the grazing angle to reduce elastic scattered ions. The blocks were mounted inside the Ciclope Scattering Chamber at a distance of around 80 cm from target. Each block covers a surface of around $9 \times 9 \text{ cm}^2$ and an active solid angle of $\sim 0.01 \text{ srad}$.

The isotopic content of the projectile $\frac{N}{Z_{\text{projectile}}} = 1.22$ has an intermediate value with respect to those of the targets $\frac{N}{Z_{^{40}\text{Ca}}} = 1.0$ and $\frac{N}{Z_{^{48}\text{Ca}}} = 1.4$. The $\frac{N}{Z}$ difference of the two Ca targets is larger than in our previous experiment [2] ($\frac{N}{Z_{\text{projectile}}} = 1.33$, $\frac{N}{Z_{^{112}\text{Sn}}} = 1.24$ and $\frac{N}{Z_{^{124}\text{Sn}}} = 1.48$) and this could enhance the effects of the isospin transport phenomena in the QP remnants.

2.1. FAZIA detector. – A FAZIA block consists of 16 telescopes mounted in a 4×4 matrix. The basic element of a block is a single telescope built according to the achievements of the R&D phase as shown in the literature [7]. It is composed of three active layers: of Si1($300\mu\text{m}$) - Si2($500\mu\text{m}$) - CsI(Tl)($\approx 10\text{ cm}$).

The signals coming from detectors are sent to the Front-End Electronics (FEE), mounted under vacuum, using a short capton cable (16 cm long) to reduce the noise contribution and they are digitized immediately after the preamplifier stage with dedicated Analog-to-Digital Converters (ADC).

During the R&D phase the FAZIA Collaboration identified the main contributions to the degradation of isotopic resolution and defined a optimized recipe to maximize the identification capability in the silicon layers:

- Usage of silicon detectors made of neutron trasmutation doped (n-TD) material to obtain a good dopant homogeneity (possibly well below 5–6%).
- Usage of silicon detectors with a thickness uniformity around $1\mu\text{m}$.
- “Random” cut of the silicon wafers with respect to the $\langle 100 \rangle$ axis of silicon lattice to avoid channeling effect all over its active area [8].
- Reverse mounting configuration of the silicon detectors (the charged fragments impinge onto the low field side of the detector) to enhance the collection time differences of the signals and identification via PSA [9].
- Usage of a thin metallization layer on both sides to reduce the sheet resistance and thus time jitter of the signals.
- FEE operated in vacuum to reduce cable lenght and noise contribution.
- Continuous monitoring bias system to mantain a constant applied voltage on each silicon detector to compensate voltage drops due to the increase of the bias current.
- Extensive optimization of digital treatment of signals.

From the reduction of the ISO-FAZIA collected data, we obtained a Z identification for all the fragments detected up to Kripton and an isotopic identification up to $Z \sim 25$ using the $\Delta E-E$ technique and up to $Z \sim 20$ with PSA with an energy threshold depending on the ion charge Z . In fig. 1 we show the nuclides chart superimposed to the identified isotopes by means of the $\Delta E-E$ method. Only fragments identified in charge and mass are shown.

3. – Preliminary results

The current status of the analysis includes the identification of fragments performed with the $\Delta E-E$ technique on Si-Si and Si-CsI matrices and the Fast-Slow identification of light particles stopped inside the CsI scintillators. The identification from PSA correlations is still in progress and therefore particles stopped inside the first silicon detector are not included in the present analysis. For this reason our energy threshold for identification is limited so far by the punch through energy of the first $\sim 300\mu\text{m}$ of silicon.

Furthermore the ^{12}C contribution due to the backing of the $^{40,48}\text{Ca}$ targets is still not taken into account and subtracted by the interesting events.

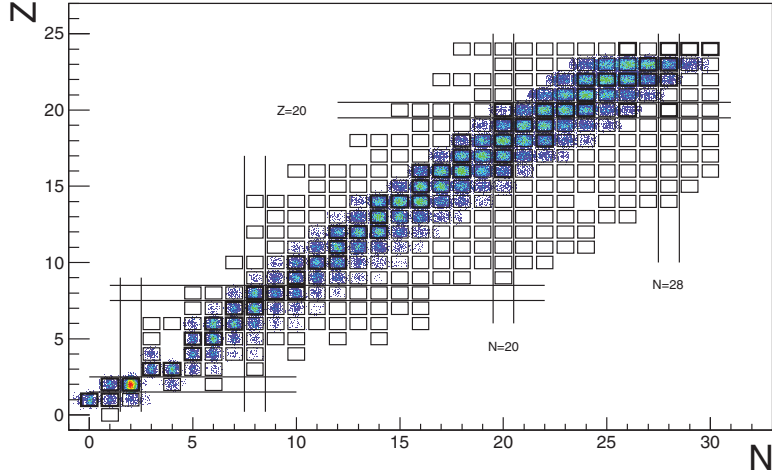


Fig. 1. – Chart of nuclides superimposed to the ISO-FAZIA identified isotopes using $\Delta E-E$ method.

In fig. 2 we show for the two studied systems the correlation between charge Z and velocity v_{lab} in the laboratory frame of the detected fragments. On the correlations we selected QP remnants using graphical cuts as indicated in fig. 2 with a black contour. In the right part of fig. 2 the charge distributions of the selected QP fragments are displayed, normalized to the same area. The two systems show a very similar distribution peaked at $Z \sim 25$ thus evidencing the selection of dissipative collisions ($Z_{projectile} = 36$).

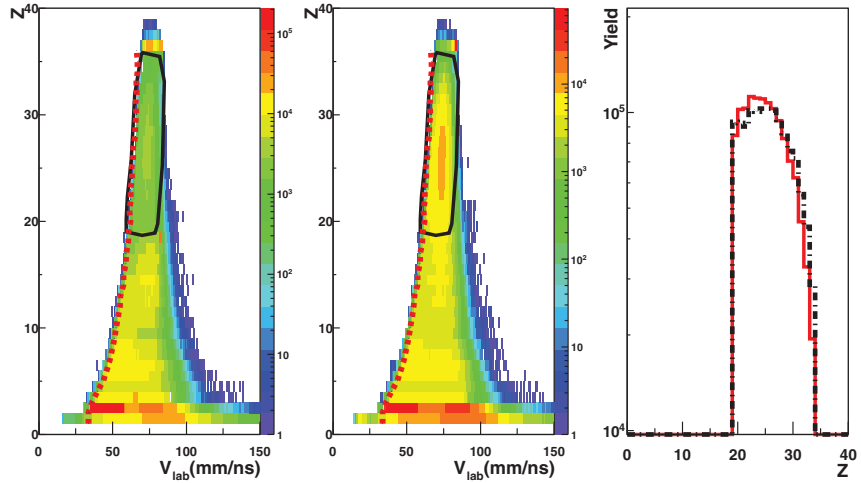


Fig. 2. – (Color online) Left panel and central panels shows the correlation between charge Z of identified fragments and their velocity in the laboratory frame for $^{80}\text{Kr} + ^{40}\text{Ca}$ (left) and $^{80}\text{Kr} + ^{48}\text{Ca}$ (middle). The black oval is the preliminary QP graphical selection and the red dashed line represents the punch through of Si1. Right panel shows the Z distribution of the QP selection for the two systems: in red continuous line the ^{40}Ca reaction and in black dashed line the ^{48}Ca .

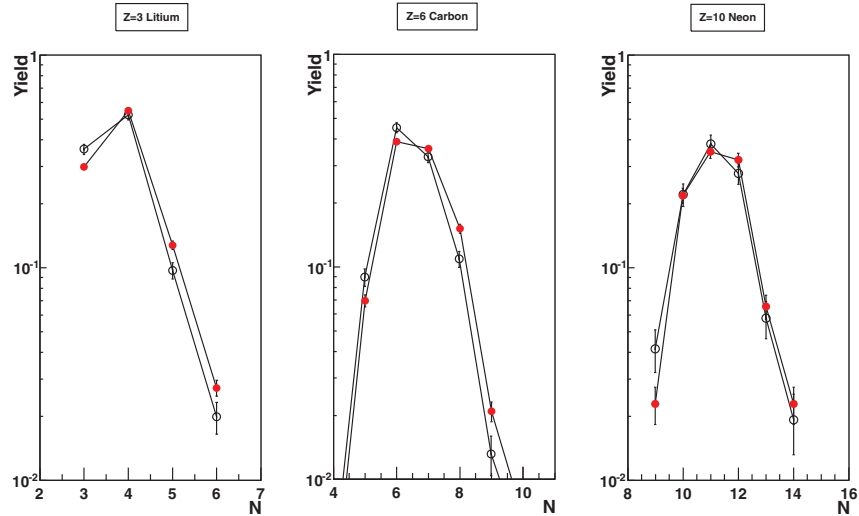


Fig. 3. – (Color online) Isotopic distribution for ions with $Z = 3$, $Z = 6$ and $Z = 10$. In red full circles the ^{48}Ca case, in black open circles the ^{40}Ca one. The ^{48}Ca reaction is always shifted toward the neutron-rich side.

We analyzed the neutron content of the fragments detected in coincidence with the selected QP. In fig. 3 we show the isotopic population of Lithium, Carbon and Neon obtained for the two investigated reactions. The distributions obtained for both systems are normalized and superimposed for the sake of comparison: in red full circles the ^{48}Ca case and in black open circles the ^{40}Ca one. It is evident that for the n-rich system the isotopic population is shifted toward the neutron rich side and this can represent a signature of the isospin diffusion process.

The $\frac{\langle N \rangle}{Z}$ values of the fragments is shown as a function of their charge Z in the panel A of fig. 4. The results are quite similar to published data [2, 3]; since the largest part of these products may come from the QP emission, this result can be interpreted as a possible evidence of isospin diffusion.

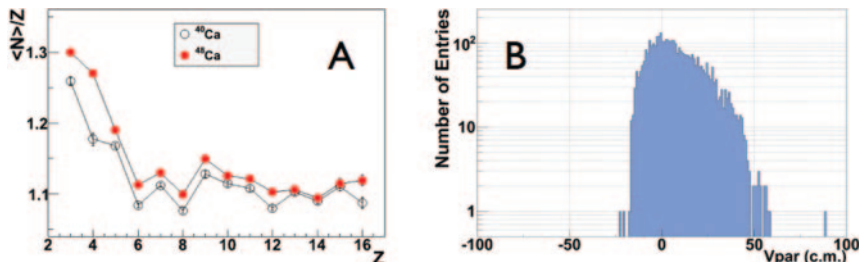


Fig. 4. – (Color online) In panel A, $\frac{\langle N \rangle}{Z}$ versus the Z for fragments for the two systems: in red full circles ^{48}Ca , in black open circles ^{40}Ca . In panel B we show for $Z = 4$ the velocity parallel to beam axis in the center of mass frame. The spectrum is peaked toward the center-of-mass origin signaling a stronger emission from the midvelocity region. The neutron enrichment of those particles could be attributed to the isospin drift effect.

Higher $\frac{\langle N \rangle}{Z}$ values are evident for lighter fragments. In panel B of fig. 4 we plotted for Berilium the parallel velocity (with respect to the beam axis) in the center of mass frame. The distribution is peaked toward the origin and this means that the main part of these products come from the midvelocity region. As a consequence, the neutron enrichment of these particles may be affected by the isospin drift phenomenon connected to the density gradient between the region of QP-QT (at normal density) and the more diluted neck zone [10, 11].

4. – Conclusion and prospectives

The FAZIA collaboration started the measurements after the R&D phase. The detector performances in terms of identification in charge and mass are even better than those obtained with the prototype telescopes. At present only particles stopped inside second silicon detector and CsI detector are included in our analysis while the identification via PSA is still in progress.

Events were a QP fragment has been detected in coincidence with some other fully identified fragments have been considered. The QP selection is performed on the Z vs. velocity correlation with graphical cuts. The preliminary results concerning $\frac{\langle N \rangle}{Z}$ for fragments detected in coincidence with QP are in good agreement with the previous published results [2, 3]; hints of effects due to the isospin diffusion and drift were found but a more deep investigation is needed.

REFERENCES

- [1] <http://fazia2.in2p3.fr/spip>
- [2] BARLINI S. *et al.*, *Phys. Rev. C*, **87** (2013) 054607.
- [3] DE FILIPPO E. *et al.*, *Phys. Rev. C*, **86** (2012) 014610.
- [4] LOMBARDO I. *et al.*, *Phys. Rev. C*, **82** (2010) 014608.
- [5] ENGLAND J. *et al.*, *Nucl. Instrum. Methods A*, **280** (1989) 291.
- [6] PAUSCH G. *et al.*, *Nucl. Instrum. Methods A*, **322** (1992) 43.
- [7] BOUGAULT R. *et al.*, *Eur. Phys. J. A*, **50** (2014) 47.
- [8] BARDELLI L. *et al.*, *Nucl. Instrum. Methods A*, **654** (2011) 272.
- [9] LE NEINDRE N. *et al.*, *Nucl. Instrum. Methods A*, **701** (2013) 145.
- [10] BARAN V. *et al.*, *Phys. Rep.*, **410** (2005) 335.
- [11] DI TORO M. *et al.*, *J. Phys. G*, **37** (2010) 083101.